SIMULATION OF REINFORCED CONCRETE BEAM-COLUMN JOINTS STRENGTHENED BY FERROCEMENT JACKETS

Bo Li and Eddie Siu-shu Lam*
Department of Civil and Environmental Engineering, The Hong Kong Polytechnic University,
Hung Hom, Kowloon, Hong Kong. *Email:cesslam@polyu.edu.hk

ABSTRACT

Beam-column joints are critical members in a moment-resisting structure to maintain the stability of the whole structure. Failure of beam-column joints is likely to cause the collapse of the structure. Many methods have been proposed to strengthen reinforced concrete beam-column joints. Among others, relocation of plastic hinges away from beam-column joints has been proved to be effective. However, there exist limited studies on numerical simulation of seismic performance of beam-column joints failed with the formation of plastic hinges at end of beams. This paper examines modeling of this type of beam-column joints using OpenSees. It is recognized that rotation due to the strain penetration of longitudinal reinforcements at the end of a plastic hinge has a substantial effect on the overall response of a beam-column joint. Omission of this effect will result in an overestimation of the hysteretic behavior. To simulate the behavior of a beam-column joint failed with the formation of plastic hinge, a numerical model based on a macro joint element combined with bond-slip zero-length element or moment-rotation spring element to account for the effect of strain penetration is proposed. This model has been successfully implemented into OpenSees for representing beam-column joints strengthened by ferrocement jackets with chamfers. It has been shown that accuracy of the numerical predictions is significantly improved by taking into account the rotation induced by strain penetration.

KEYWORDS

Beam-column joints, OpenSees, strain penetration, ferrocement, strengthening.

INTRODUCTION

In moment-resisting structures, beam-column joints have been recognized as critical members for transferring forces and moments among the beams and the columns. Under seismic action, beam-column joints transfer higher shear forces as compared with the adjoining members due to the moment reversal across the joints. Thus, beam-column joints should be designed to have sufficient shear strength in order to maintain the stability and integrity of the structures.

Buildings in areas of low to moderate seismic risk, such as those in Hong Kong, were traditionally designed without seismic provisions, i.e. designed to gravity load and wind load only (Lam et al. 2002). Beam-column joints designed without seismic provision or detailing are normally in lack of transverse reinforcements or without adequate confinement in the joint cores. Figure 1 shows examples of standard method of detailing reinforced concrete beam-column joints (IStructE 1989). Transverse reinforcements are not provided in the joint. Horizontal load to be considered is only wind loading. Concerning low- to medium-rise buildings, wind effect is very small as compared with possible earthquake effect. As a result, buildings performing well under conventional load cases may suffer some degrees of damage under earthquake, which depends on the intensity of the earthquake. Proper strengthening is required to enhance seismic performance of non-seismically designed structures. More seriously, failure of beam-column joints in moment-resisting structures may cause catastrophic collapse of buildings (Kam et al. 2011). Strengthening is necessary and preferable to improve seismic behavior of non-seismically designed beam-column joints (Algirdas 2002).

Proper consideration of joint flexibility in frame structures is essential to capture the overall performance of a structure under earthquake action. Previous studies have demonstrated the importance of joint flexibility for assessment of reinforced concrete structures. Ghobarah and Biddah (1999) performed dynamic analyses of RC frames with flexible joint or rigid joint. It was concluded that incorporation of inelastic shear deformation in the joints had a significant influence on the seismic performance of structure. Overall displacement response of the frame increased when including joint flexibility. Karayannis et al. (2011) investigated the influence of strength and stiffness degradation in exterior joints on the local and global failure mechanisms of RC structures.

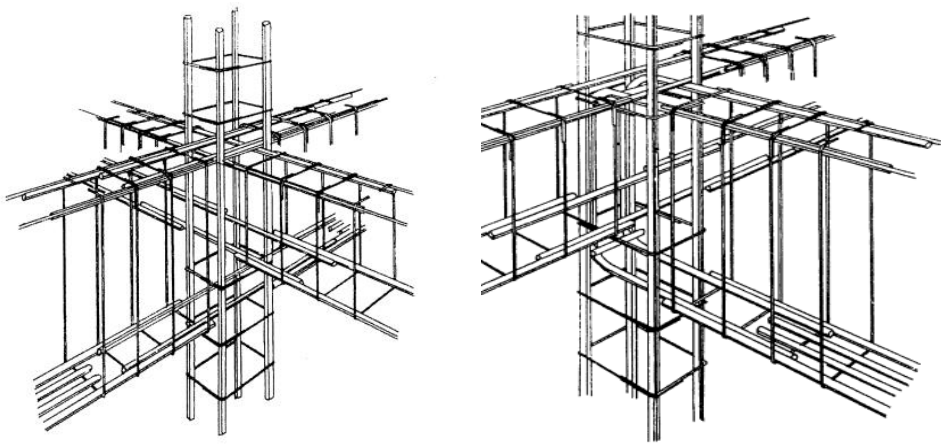

Figure 1 Traditional beam-column joints in Hong Kong (IStructE 1989)

Response of the structures with and without joint degradation demonstrated that neglecting the possible local damage of exterior joints may lead to erroneous assessment of seismic behavior. Park and Mosalam (2013) compared the nonlinear dynamic response of three hypothetical non-ductile RC buildings considering or ignoring joint flexibility. It revealed a significant difference in spectral accelerations at 2.0% drift for building structures with and without joint flexibility. Conventional ways of modelling a frame structure, however, rarely incorporate joint flexibility and consider the joints as rigid elements. A reliable, practical approach for modelling various types of beam-column joints is needed.

This paper presents a study on numerical simulation of beam-column joints strengthened by ferrocement jackets, especially for those failed with the formation of plastic hinges in the beam. This type of failure is beneficial to resist earthquake for a frame structure. A numerical model based on macro joint element and bond-slip zero-length element or moment-rotation spring element is proposed. Details of the proposed beam-column joint model and some of the results obtained using the proposed model are presented. The model has been implemented into OpenSees as zero-length sectional element or spring element at the end of a plastic hinge. Finally, results obtained from the numerical simulation are compared with the test results.

SIMULATION OF BEAM-COLUMN JOINTS

Simulation is conducted on reinforced concrete beam-column joints using OpenSees (2009). OpenSees is an object-oriented, open-source software framework for simulating the seismic response of structural and geotechnical members and systems. A macro joint element proposed by Lowes et al. (2003) is adopted to simulate the behavior of joint core. Beam-column joints with and without strengthening tested by the authors are selected for simulation (Li et al. 2015). Figure 2 shows the strengthened exterior beam-column joints. Boundary conditions are identical to those used in the tests. Constant axial load is first applied. Subsequently, horizontal load is applied at the beam tip using displacement control.

Macro Joint Element

A macro model available in OpenSees (2009) is employed to simulate the response of RC beam-column joints under cyclic loading. As shown in Figure 3, the element ("BeamColumnJoint" element) consists of one shear panel element, eight bar-slip springs and four interface-shear springs. Shear panel elements are used to simulate strength and stiffness degradation due to failure of the joint core. Bar-slip springs simulate stiffness and strength degradation due to anchorage-zone damage. Interface shear spring simulates the reduced capacity of shear transfer at the joint perimeter due to crack opening.

Generally, cross-section of un-strengthened joint is divided into confined concrete core and unconfined concrete cover with consideration of confinement provided by transverse reinforcements. For a beam-column joint strengthened by ferrocement jacket, the cross-section is discretized into confined concrete core, confined mortar and unconfined mortar. Stress-strain relationship of confined concrete is determined according to modified Kent-Park model (Scott et al. 1982). "Concrete02" available in OpenSees is adopted to represent concrete and mortar fibers. For simplicity, "Steel02" model with a bilinear monotonic stress-strain curve is used for reinforcing steel and wire mesh. Envelop of shear stress-strain relationship for shear panel zone is determined

based on the test results (Li et al. 2015) and is implanted using "pinching4". Other parameters related to unloading and reloading are defined as follows. rDispP and rDipsN are equal to 0.25. rForceP and rForceN are set to be 0.3. To include P-Δ effect, different values are used for uForceP and uForceN at various axial loads. In this study, uForceP (or uForceN) is -0.2 for the specimens under $0.2f_c'A_g$ axial load.

Figure 2 Exterior beam-column joint strengthened by ferrocement jackets with chamfers

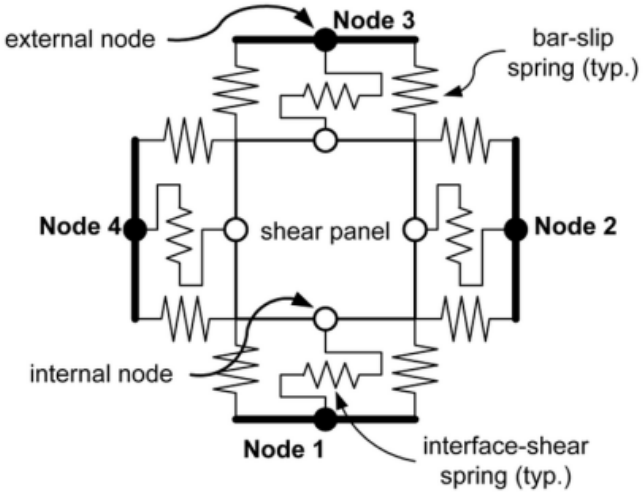

Figure 3 Macro beam-column joint element (Lowes et al. 2003)

Beam-Column Joints

Two exterior beam-column joints (Specimens JC0 and JS2) in the authors' study (Li et al. 2015) are selected. They represent two types of failure mechanisms: joint-shear failure and beam-flexural failure. Details of specimens can be referred to Li et al. (2015). A schematic view of the beam–column joint model and discretization of cross-section in the control specimen is given in Figure 4. For specimen JS2, joint core is enlarged after installing chamfers at beam-column corners. In the simulation, joint core is divided into two parts, including joint shear panel considered in "BeamColumnJoint" element and "Beamcolumn" element with varying cross section. Here, chamfer region is modeled by four "Beamcolumn" elements with the cross-section reduced linearly with depth, from 500 mm to 200 mm. Besides, ferrocement jackets are also included by specifying appropriate sectional properties. A schematic model for a beam-column joint strengthened by ferrocement jacket with chamfers is given in Figure 5. "BeamwithHinges" element is adopted to model possible plastic hinge zone.

Extent of plasticity for the specimen failed in beam-flexural is controlled by the length of plastic hinge. Scott and Fenves (2006) compared two methods of computing the length of plastic hinge: 0.216L based on Paulay and Priestley (1992) (i.e. based on equations (1) to (3) from Priestley et al. 2007) and 0.226L by Coleman and

Spacone (2001). Here, L is the length of a member. It was concluded that close agreement was attained using the two methods for global load-displacement response and local moment-curvature response of a reinforced concrete bridge pier. Thus, an empirical method for calculating length of plastic hinge is adopted (Priestley et al. 2007) using in the following equations.

$$L_p = kL_c + L_{sp} \geq 2L_{sp} \tag{1}$$

$$k = 0.2\left(\frac{f_u}{f_y} - 1\right) \leq 0.08 \tag{2}$$

$$L_{sp} = 0.022 f_y d_b \tag{3}$$

where L_p, L_{sp} and L_c are the plastic hinge length, the strain penetration length and the cantilever member length respectively (in mm); f_y and f_u are yield strength and ultimate stress of longitudinal reinforcements respectively (in MPa). d_b is the diameter of longitudinal reinforcement (in mm). Calculated plastic hinge length for this study is about 175 mm.

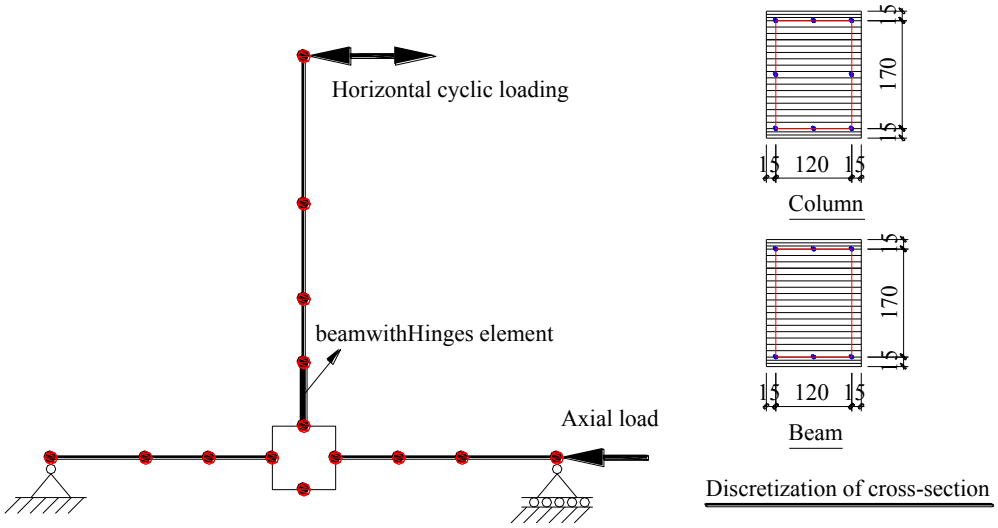

Figure 4 Numerical model of exterior beam-column joints

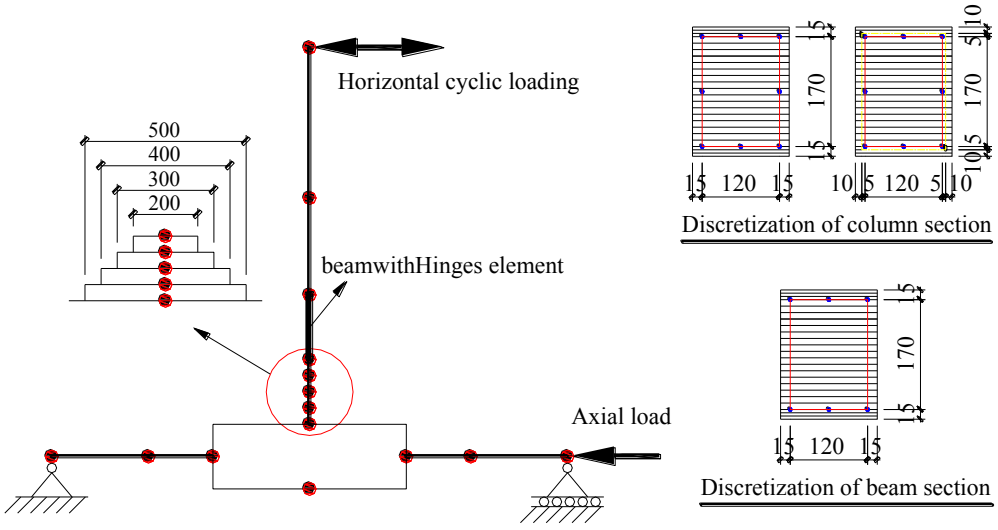

Figure 5 Numerical model of exterior joint strengthened by ferrocement jackets with chamfers

RESULTS AND DISCUSSIONS

Shear-Failure Specimen

Figure 6 compares simulation with test results for specimen JC0. The tested and predicted lateral loads are 25.5 kN and 26.3 kN respectively. In the negative direction, the tested and predicted lateral loads are 23.6 kN and 26.2 kN respectively. Lateral load in positive direction is well predicted while that in negative direction is overestimated. This is attributed to the use of symmetrical constitutive material model for shear panel zone. Furthermore, post-peak load at beam tip is overestimated. This is attributed to in lack of consideration in concrete spalling at the advanced stage of loading (Panagiotakos and Fardis 2001). Generally, main characteristics of hysteretic load-displacement curve are captured in the simulation of specimen JC0.

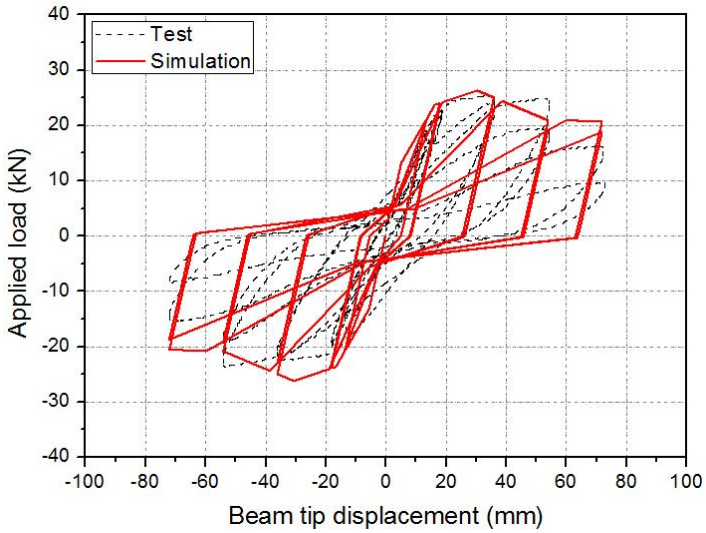

Figure 6 Comparison of simulation with test result for specimen JC0

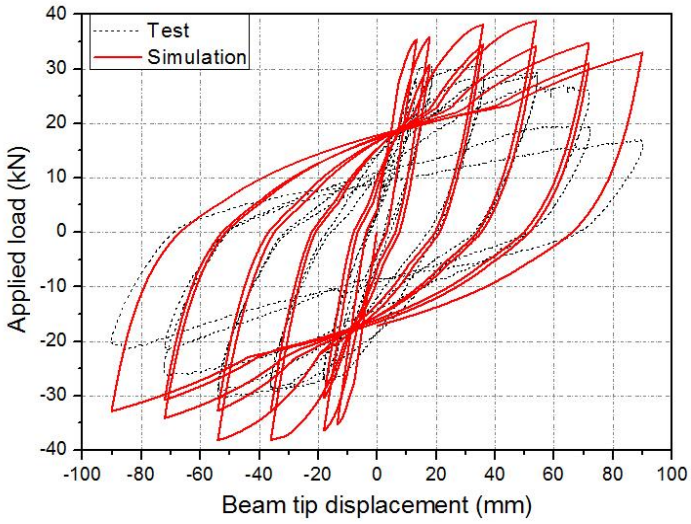

Figure 7 Comparison of simulation with test result for specimen JS2 without consideration on strain penetration

Flexural-Failure Specimen

Figure 7 shows the comparison of simulation with test result for specimen JS2 without consideration on strain penetration at end of plastic hinge. The tested lateral loads in push and pull directions are 30.9 kN and 30.3 kN respectively. Applied load at beam tip is overestimated at 38.8 kN in push direction and 38.2 kN in pull direction in the simulation. This may be attributed to possible error in considering plastic hinge in the beam.

Stain penetration normally occurs at the end of plastic hinge. Simulation of RC columns has demonstrated that without considering strain penetration effect may significantly overestimate post-peak strength. Besides, fixed-end rotation contributed approximately 25%-40% of the total horizontal displacement for both RC circular columns and rectangular columns (Lehman and Moehle 2000; Sezen and Moehle 2006; Feng 2013). In this study, strain penetration is observed with cracking at chamfers in the strengthened joints. However, fiber section beam-column elements do not take into account fixed-end rotation due to the strain penetration of longitudinal reinforcements. A joint failed in beam flexural has similar support condition as a cantilever column. Thus, modeling of beam-column joints should include strain penetration at plastic hinge zones. Two approaches for considering strain penetration are examined, including the use of a zero-length section element with bond slip behavior and a zero-length spring element with moment-rotation relationship.

Bond-slip at interface

Strain penetration at the end of plastic hinge is introduced by including a bond-slip relationship for longitudinal reinforcements. As shown in Figure 8, a zero-length fiber section containing bond-slip relationship is inserted at the interface between strengthened and un-strengthened area. This sectional element has the same reinforcement detail for which the constitutive relationship is defined by a hysteretic stress-slip model containing strain penetration effect. Zhao and Sritharan (2007) proposed a material model "Bond_SP01" to reflect stress-slip relationship of longitudinal reinforcements. They highlighted that the model is applicable to fully anchored reinforcement. This is consistence with beam reinforcement detail in the strengthened joint.

Comparison of simulation using a model with zero-length fiber section and test data for specimen JS2 is shown in Figure 9. Prediction in terms of applied load versus displacement at beam tip agrees with test result in terms of peak load, displacement corresponding to peak strength and strength degradation. The predicted lateral loads in push and pull directions are reduced to 31.9 kN and 32.1 kN respectively. Furthermore, descending segment in load-displacement curve is captured in the simulation. It is noted that non-symmetrical response in push and pull direction is not considered in the simulation. The main deficiency in the simulation is at the advanced stage of loading in that load increases gradually as displacement increases. This may be attributed to the spalling of concrete and buckling of longitudinal reinforcements (Panagiotakos and Fardis 2001). Such phenomenon is observed in the test but not considered in the simulation.

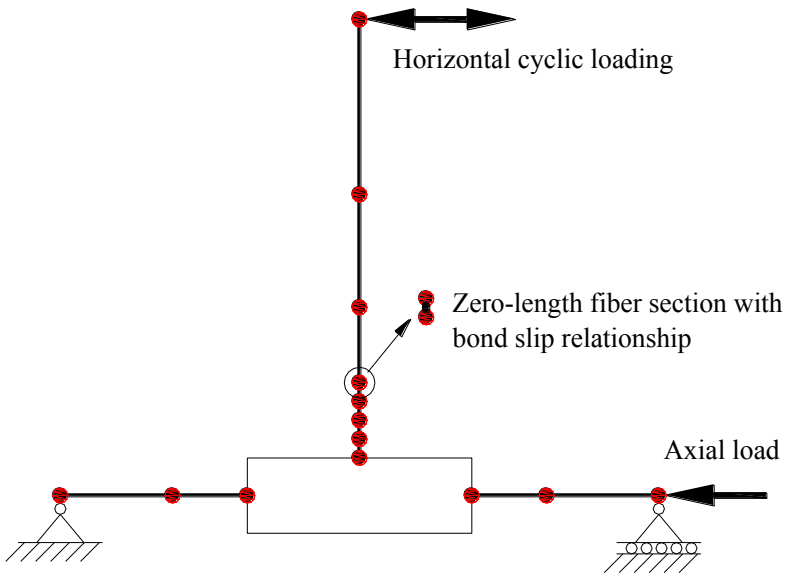

Figure 8 Numerical model of ferrocement-strengthened joint with zero-length fiber section

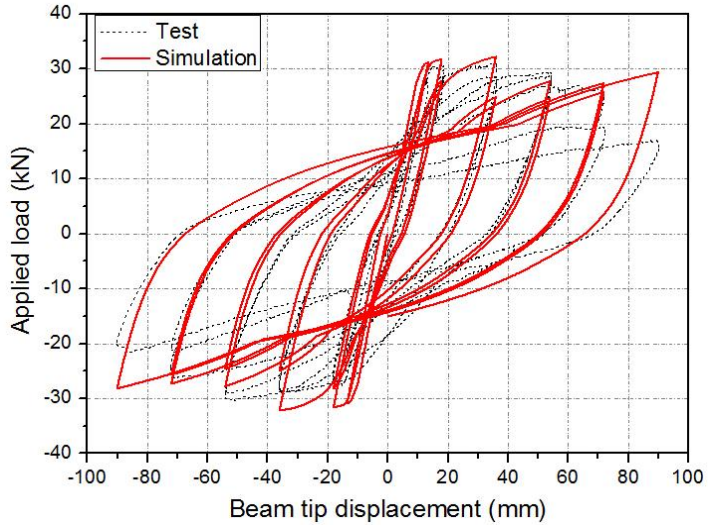

Figure 9 Comparison of simulation with test result for specimen JS2 with strain penetration using zero-length fiber section

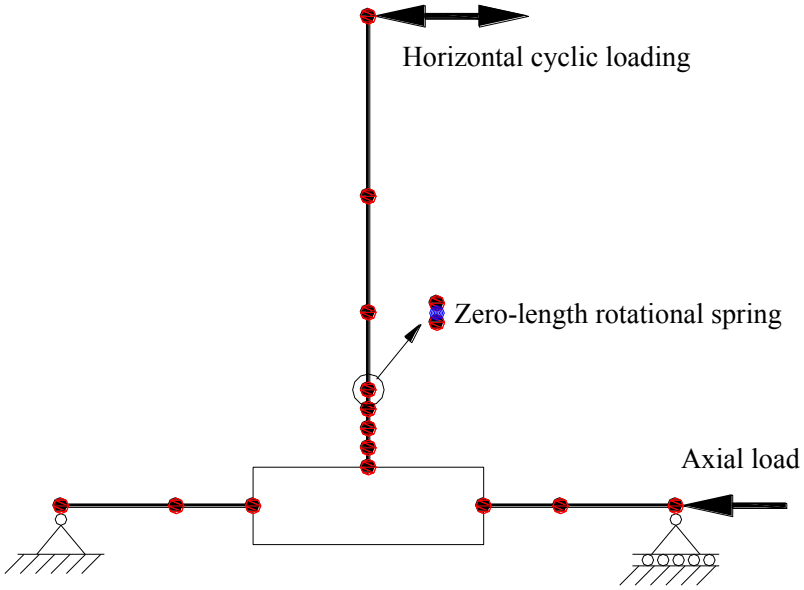

Figure 10 Numerical model of ferrocement-strengthened joint with zero length rotation spring element

Rotational spring

Strain penetration at the end of plastic hinge is also modeled through a rotational spring. The rotational spring reflects total moment-rotation relationship at end of plastic hinge. Thus, a zero-length spring element is added at the interface of strengthening area to un-strengthening area as shown in Figure 10. Constitutive model for rotational spring is defined and discussed as follows.

There are a number of hysteretic models for simulating cyclic deterioration in strength and stiffness of RC members (Otani 1981; Sivaselvan and Reinhorn 2000; Ibarra et al. 2005). Among others, modified Ibarra-Medina-Krawinkler (IMK) model is adopted to simulate constitutive relationship for rotational spring in this study. This model is able to simulate strength deterioration with a descending slope after reaching the load bearing capacity of a structural member. This is one of the key features of the IMK model as compared with traditional models, such as simple bilinear models. The IMK model simulates up to four modes of cyclic deterioration including strength degradation, post-peak strain softening, unloading stiffness degradation, and accelerated reloading stiffness deterioration (Ibarra et al. 2005). Cyclic deterioration is based on normalized energy dissipation capacity and an exponent factor that describes the rate of cyclic deterioration against

accumulation of damage (Ibarra et al. 2005). This model is implemented in OpenSees as shown in Figure 11.

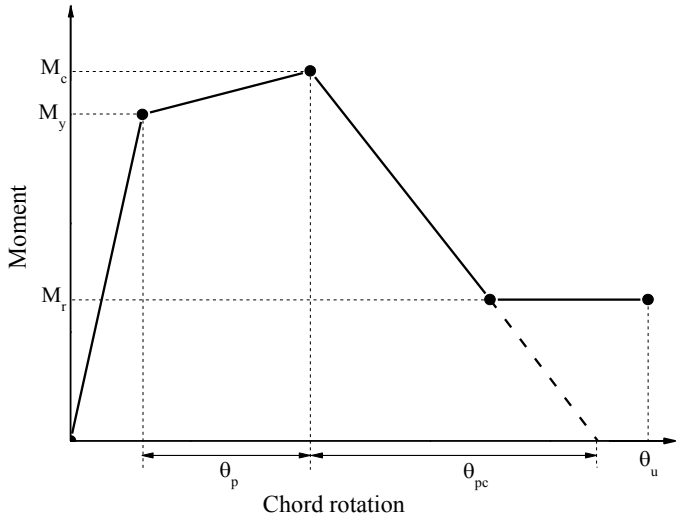

Figure 11 Envelop of IMK model

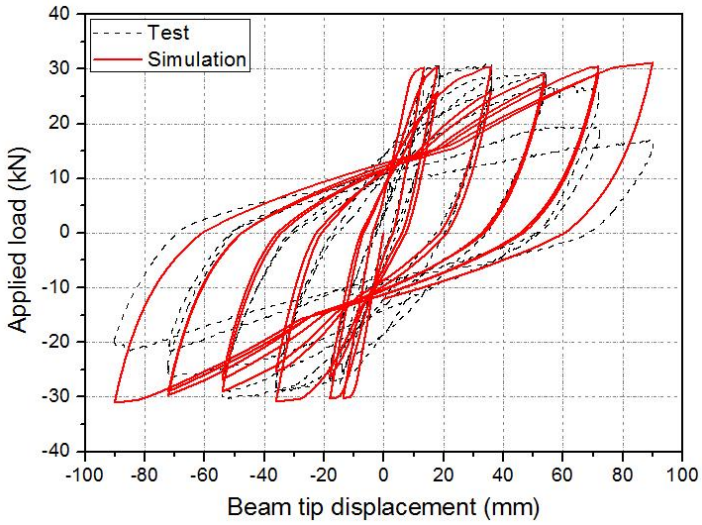

Figure 12 Comparison of simulation using rotational spring with test result for specimen JS2

Seven parameters are required to control the monotonic and cyclic performance of the IMK model. There are yield moment, chord rotation at yield, chord rotation at peak moment, hardening stiffness ratio, post-capping stiffness, normalized hysteretic energy dissipation index and an exponent term to model the rate of deterioration. Haselton et al. (2008) calibrated IMK model using 255 RC columns and considered the influence of axial load, transverse reinforcement ratio, arrangement of transverse reinforcement and concrete. Based on database, prediction formulas for determining parameters in IMK model were proposed in equations (4) to (8).

Flexural strength at yielding is determined according to the prediction proposed by Panagiotakos and Fardis (2001). It has been proved to provide adequate accuracy in predicting flexural strength. Predictive equations proposed by Haselton et al. (2008) are adopted to define the parameters in IMK model as shown in Equations (4) to (8). Equation (4) is the secant stiffness. Equation (5) illustrates strain hardening ratio for positive (negative) loading direction. Cyclic deterioration parameters for strength, post-capping strength, reloading stiffness and unloading stiffness are predicted using Equation (6). Pre-capping chord rotation and post capping chord rotation for positive (negative) loading direction are calculated using Equations (7) and (8) respectively. It is worth noticing that rate of deterioration for each parameter is equal to default value at 1.0.

$$\frac{EI_y}{EI_g} = 0.065 + 1.05v \quad 0.2 \le \frac{EI_y}{EI_g} \le 0.6 \tag{4}$$

$$M_c / M_y = (1.25)(0.89)^n (0.91)^{0.01 f_c'} \tag{5}$$

$$\lambda = (170.7)(0.27)^n (0.10)^{s/d} \tag{6}$$

$$\theta_p = 0.13(1 + 0.55\alpha_{sl})(0.13)^n (0.02 + 40\rho_{sh})^{0.65} (0.57)^{0.01 f_c'} \tag{7}$$

$$\theta_{pc} = (0.76)(0.031)^n (0.02 + 40\rho_{sh})^{1.02} \tag{8}$$

where EI_y and EI_g are the effective cross-sectional moment of inertia and the gross cross-sectional moment of inertia respectively. M_c and M_y are the capping moment capacity and the yielding moment respectively; n is the axial load ratio of the member; s/d is the ratio of stirrup spacing and the depth of the section; ρ_{sh} is the area ratio of transverse reinforcement in the plastic hinge region. α_{sl} is the bond-slip indicator (equal to 1.0 where bond-slip is possible and equal to 0 where bond-slip is not possible).

Using the model with rotational spring element, predicted result of specimen JS2 is plotted in Figure 12 and is compared with test result as shown in dash line. Hysteretic load-displacement curve is accurately predicted. The predicted lateral load is 30.3 kN in push direction and 30.8 kN in pull direction. Similar to the simulation with zero-length fiber section, the applied load is overestimated at final stage of loading. This may be attributed to that buckling of longitudinal reinforcement and spalling of concrete are not taken into account in the simulation (Panagiotakos and Fardis 2001). Generally, parameters of IMK model are obtained from regression analysis.

CONCLUSIONS

Numerical simulation of reinforced concrete exterior beam-column joints with and without strengthening is developed using OpenSees. Response of non-seismically designed beam-column joints can be predicted when proper constitutive relationship is defined for joint shear panel. Numerical simulation on the strengthened joint is focused on modeling the plastic hinge as the joint failed in beam-flexural. Two methods are used to represent strain penetration effect at the end of plastic hinge, including adopting bond-slip relationship and moment-rotation spring element. The methods improve the predictions for beam-column joints failed in beam-flexural. However, overestimation of loading is found in both models at the advanced stage of loading. This may be attributed to the lack of considerations in buckling of longitudinal reinforcements and spalling of concrete. Further studies are needed to refine the material models for reinforcing steel. In addition, determination of parameters in “Pinching4” and “IMK” necessaries further study as most of them are obtained empirically.

ACKNOWLEDGMENTS

The authors gratefully acknowledge the financial support provided by the Research Grants Council of Hong Kong (RGC No.: PolyU 5206/08E) and Construction Industry Institute (Hong Kong) / PolyU Innovation Fund (No.: 5-ZJHH). The authors would like to thank for the technical assistance provided by the Structural Engineering Research Laboratory of the Hong Kong Polytechnic University.

REFERENCES

Algirdas, K. (2002). "Structural behaviour of joints of multi-storey concrete buildings." Monograph. Vilnius: Technika, 128 p..

Coleman, J., and Spacone, E. (2001). "Localization issues in force-based frame elements." Journal of Structural Engineering-ASCE, 127(11), 1257–1265.

Feng, Y.H. (2013). "Numerical simulation and analysis of circular reinforced concrete bridge columns for investigating the effect of seismic load history on longitudinal bar buckling." PhD thesis, North Carolina State University.

Ghobarah, A., and Biddah, A. (1999). "Dynamic analysis of reinforced concrete frames including joint shear deformation." Engineering Structures, 21(11), 971-987.

Haselton, C.B., Liel, A.B. Lange, S.T., and Deierlein, G.G. (2008). "Beam-column element model calibrated for predicting flexural response leading to global collapse of RC frame buildings." PEER Report 2007/03.

Ibarra, L.F., Medina, R., and Krawinkler, H. (2002). "Hysteretic models that incorporate strength and stiffness deterioration." Earthquake Engineering and Structural Dynamics, 34(12), 489-1511.
IStructE (1989). "Standard method of detailing structural concrete." The Institution of Structural Engineers, The Concrete Society, 138pp.
Kam, W.Y., Pampanin, S., and Elwood, K. (2011). "Seismic performance of reinforced concrete buildings in the 22 February Christchurch (Lyttelton) earthquake." Bulleten of The New Zealand Society for Earthquake Engineering, 44, 239-78.
Karayannis, C.G., Favvata, M.J., and Kakaletsis, D.J. (2011). "Seismic behaviour of infilled and pilotis RC frame structures with beam-column joint degradation effect." Engineering Structures, 33(10), 2821-2831.
Lam, S. S. E., Xu, Y. L., Chau, K. T., Wong, Y. L., and Ko, J. M. (2002). "Progress in earthquake resistant design of buildings in Hong Kong." Proceedings of the Structural Engineers World Congress (SEWC2002), Oct 9-12, 2002, Yokohama, Japan.
Lehman, D.E., and Moehle, J.P. (2000). "Seismic performance of well-confined concrete bridge columns." PEER Report 1998/01, Pacific Earthquake Engineering Research Center.
Li, B., Lam E.S.S., Cheng Y.K., Wu B. and Wang Y.Y. (2015) "Strengthening of non-seismically designed beam-column joints by ferrocement jackets with chamfers". Earthquakes and Structures, 8(5), 1017-1038.
Lowes, L.N., Mitra, N., and Altoontash, A. (2003). "A beam-column joint model for simulating the earthquake response of reinforced concrete frames." PEER-2003/10.
Otani, S. (1981). "Hysteresis models of reinforced concrete for earthquake response analysis." J. Fac. Eng. Univ. Tokyo, XXXVI(2), 407–441.
OpenSees (2009). Open System for Earthquake Engineering Simulation. Pacific Earthquake Engineering Research Center, University of California, Berkeley. http://opensees.berkeley.edu.
Park, S., and Mosalam, K.M. (2013b). "Simulation of reinforced concrete frames with nonductile beam-column joints." Earthquake Spectra, 29(1), 233-257.
Paulay, T., and Priestley, M.J.N. (1992). "Seismic design of reinforced concrete and masonry buildings." John Wiely & Sons, INC.
Panagiotakos, T.B. and Fardis, M.N. (2001) "Deformations of reinforced concrete members at yielding and ultimate." ACI Structural Journal, 98(2), 135-148.
Priestley, M.J.N., Calvi, G.M., and Kolwasky, M.J. (2007). "Displacement-based seismic design of structures." IUSSS Press, Pavia, Italy.
Scott, B.D., Park, R., and Priestley, M.J.N. (1982). "Stress-strain behavior of concrete confined by overlapping hoops at low and high-strain rates." Journal of the American Concrete Institute, 79(1), 13-27.
Scott, M.H., and Fenves, G.L. (2006). "Plastic hinge integration methods for force-based beam-column elements." Journal of Structural Engineering, 132(2), 244-252.
Sezen, H., and Moehle, J.P. (2006) "Seismic tests of concrete columns with light transverse reinforcement." ACI Structural Journal, 103(6), 842-849.
Sivaselvan, M., and Reinhorn, A.M. (2000). "Hysteretic models for deteriorating inelastic structures." Journal of Engineering Mechanics, 126(6), 633–640.
Zhao, J., and Sritharan, S. (2007). "Modeling of strain penetration effects in fiber-based analysis of reinforced concrete structures." ACI Structural Journal, 104(2), 133-141.